Biogeosciences Discuss., 11, 14489–14530, 2014
www.biogeosciences-discuss.net/11/14489/2014/
doi:10.5194/bgd-11-14489-2014

Biogeosciences Discussions
Open Access

Pigment signatures of phytoplankton communities in the Beaufort Sea

P. Coupel[1], A. Matsuoka[1], D. Ruiz-Pino[2], M. Gosselin[3], H. Claustre[4], D. Marie[5], J.-É. Tremblay[1], and M. Babin[1]

[1]Joint International ULaval-CNRS Laboratory Takuvik, Québec-Océan, Département de Biologie, Université Laval, Québec, Québec G1V 0A6, Canada
[2]Laboratoire d'Océanographie et du Climat: Expérimentation et Approches Numériques (LOCEAN), UPMC, CNRS, UMR7159, Paris, France
[3]Institut des sciences de la mer de Rimouski (ISMER), Université du Québec à Rimouski, 310 allée des Ursulines, Rimouski, Québec, G5L 3A1, Canada
[4]Laboratoire d'Océanographie de Villefranche (LOV), CNRS and Université Pierre et Marie Curie, UMR7093, Villefranche-sur-Mer, France
[5]Station Biologique, CNRS, UMR7144, INSU et Université Pierre et Marie Curie, Place George Teissier, 29680 Roscoff , France

Received: 11 August 2014 – Accepted: 9 September 2014 – Published: 13 October 2014

Correspondence to: P. Coupel (pierre.coupel@takuvik.ulaval.ca)

Published by Copernicus Publications on behalf of the European Geosciences Union.

Abstract

Phytoplankton are expected to respond to recent environmental changes of the Arctic Ocean. In terms of bottom-up control, modifying the phytoplankton distribution will ultimately affect the entire food web and carbon export. However, detecting and quantifying change in phytoplankton communities in the Arctic Ocean remains difficult because of the lack of data and the inconsistent identification methods used. Based on pigment and microscopy data sampled in the Beaufort Sea during summer 2009, we optimized the chemotaxonomic tool CHEMTAX for the assessment of phytoplankton community composition in an Arctic setting. The geographical distribution of the main phytoplankton groups was determined with clustering methods. Four phytoplankton assemblages were determined and related to bathymetry, nutrients and light availability. Surface waters across the whole survey region were dominated by prasinophytes and chlorophytes, whereas the subsurface chlorophyll maximum was dominated by the centric diatoms Chaetoceros socialis on the shelf and by two populations of nanoflagellates in the deep basin. Microscopic count showed a high contribution of the heterotrophic dinoflagellates Gymnodinium and Gyrodinium spp. to total carbon biomass, suggesting high grazing activity at this time of the year. However, CHEMTAX was unable to detect these dinoflagellates because they lack peridinin. The inclusion in heterotrophic dinoflagellates of the pigments of their prey potentially leads to incorrect group assignments and some misinterpretation of CHEMTAX. Thanks to the high reproducibility of pigment analysis, our results can serve as a baseline to assess change and spatial or temporal variability in phytoplankton populations.

1 Introduction

The Arctic environment experiences transformations caused by climate change highlighted by the accelerating reduction of the summer sea ice extent (Comiso et al., 2008; Rothrock et al., 1999; Stroeve et al., 2011). Rapid response of phytoplankton in terms

BGD
11, 14489–14530, 2014

of diversity and dominance has already been discussed (Carmack and Wassmann, 2006). A shift towards smaller sized phytoplankton was suggested in the Canadian Arctic as a result of low nitrate availability and strong stratification (Li et al., 2009). A recent study suggested that nanoflagellates would be promoted in the newly ice free basins as a consequence of the deepening nitracline (Coupel et al., 2012). More frequent wind-driven upwelling events could multiply the production and favour the development of large taxa such as diatoms (Pickart et al., 2013; Tremblay et al., 2011). The earlier ice retreat may affect the zooplankton and benthos by altering the timing and location of the spring bloom and associated species succession (Grebmeier et al., 2010; Hunt Jr et al., 2002). In response to these changes, a reorganization of the Arctic Ocean food web would be expected causing changes in the function of the ecosystem and ultimately fisheries but also on biogeochemical cycles (Falkowski, 2000) and carbon export (Sigman and Boyle, 2000; Wassmann and Reigstad, 2011).

Monitoring the diversity and dominance of Arctic phytoplankton is a prerequisite to document change. However, it is very difficult to detect responses of phytoplankton in the Arctic due to a lack of quantitative information on taxonomic composition (Poulin et al., 2010; Wassmann et al., 2011). Moreover, the various and inconsistent approaches used for phytoplankton identification strongly limit intercomparisons between different datasets. A reproducible method to monitor phytoplankton communities needs to be established. Optical microscopy is a good option to identify and enumerate large phytoplankton but the procedure is expensive, time-consuming and relies greatly on the skill of the taxonomist (Wright and Jeffrey, 2006). Other techniques are better suited to identify small phytoplankton (Ansotegui et al., 2001; Roy et al., 1996; Schlüter et al., 2000). The remote sensing approach is becoming increasingly attractive with the recent advances in the interpretation of optical signals to detect diatoms and other phytoplankton groups from space (Alvain et al., 2005; Hirata et al., 2011; Sathyendranath et al., 2004; Uitz et al., 2006). However, the satellite method is restricted to the surface layer and is still limited by the presence of sea ice, frequent cloudy conditions and coastal turbidity in the Arctic Ocean (IOCCG, 2014).

BGD
11, 14489–14530, 2014

The use of pigments as markers of major phytoplankton groups is a good candidate to monitor Arctic phytoplankton although being limited by the acquisition of water samples during oceanographic cruises. Automated measurements of pigment concentrations using high performance liquid chromatography (HPLC) allows fast and highly reproducible analyses (Jeffrey et al., 1997). Moreover, pigment analysis allows to characterize both the large and small size phytoplankton (Hooker et al., 2005). The main issue when using pigments for quantitative taxonomy is the overlap of several pigments among phytoplankton groups. The chemotaxonomic software CHEMTAX was developed to overcome this problem by considering a large suite of pigments simultaneously (Mackey et al., 1996). CHEMTAX has been widely used in the global ocean, notably in Antarctic polar waters (Kozlowski et al., 2011; Rodriguez et al., 2002; Wright et al., 1996).

Only few studies have used CHEMTAX in the Arctic Ocean to date. Spatial and temporal variability of the phytoplankton community structure were described for the North Water Polynya (Vidussi et al., 2004) and the Canada Basin (Coupel et al., 2012; Taylor et al., 2013), while Alou-Font et al. (2013) used CHEMTAX to describe the influence of snow conditions on the sea-ice communities of Amundsen Gulf. Phytoplankton communities were also investigated using CHEMTAX in subarctic regions, i.e. the Bering Sea (Suzuki et al., 2002) and in the Faroe-Shetland channel (Riegman and Kraay, 2001). Investigations of the reliability of CHEMTAX underscored the need to adapt procedures to the targeted area by investigating the dominant species, their pigment content and the environmental conditions such as light availability and nutrient status (Wright and Jeffrey, 2006). Despite this caveat most prior studies using CHEMTAX in Arctic Ocean have used a parameterization made for Antarctic waters. Inappropriate parameterization of CHEMTAX has been identified as the main source of misinterpretation in taxonomic determinations based on pigments (Irigoien et al., 2004; Lewitus et al., 2005). An Arctic-specific parameterization of CHEMTAX is thus required before using it to examine possible changes in the phytoplankton community structure.

BGD
11, 14489–14530, 2014

The objective of this study was to examine Arctic phytoplankton community structure by CHEMTAX using samples collected during summer in the Beaufort Sea. This region, which is influenced by freshwater from the Mackenzie River over the narrow continental shelf and by oceanic waters and ice-melt waters in the deep ocean basin, allowed us to test the performance of CHEMTAX under diverse environmental conditions. Accurate taxonomic identification and enumeration of cells > 3 µm were combined with flow-cytometric sorting and counting of picophytoplankton cells (1–3 µm) to identify the dominant phytoplankton groups. Then the pigment ratios of these dominant Arctic groups were found in the literature and used to tune the CHEMTAX software. The development of tools like CHEMTAX is critical to investigating changes in populations over time.

2 Materials and methods

Hydrographical observations and seawater sampling were carried out in the Beaufort Sea (69–73° N; 125–145° W) during Leg 2b of the MALINA cruise in summer 2009 (30 July to 27 August 2009) onboard the CCGS *Amundsen*. Twenty stations were sampled on the Mackenzie shelf and the deep waters of the Beaufort Sea (Fig. 1) using Niskin-type bottles mounted on a CTD-Rosette system equipped with sensors to measure photosynthetically active radiation (PAR; Biospherical QCP-2300), temperature and salinity (Sea-Bird SBE-911plus). Phytoplankton communities were investigated using three different approaches: pigment signature (386 samples), light microscopy (88 samples) and flow cytometry (182 samples).

2.1 Pigments

We followed the HPLC analytical procedure proposed by Van Heukelem and Thomas (2001). Briefly, photosynthetic phytoplankton pigments were sampled at 6 to 10 depths in the upper 200 m of the water column, however only samples from the surface (5 m)

BGD
11, 14489–14530, 2014

and sub-surface chlorophyll *a* maximum (SCM) are presented in this work. Seawater aliquots ranging from 0.25–2.27 L were filtered through 25 mm Whatman GF/F filters (nominal pore size of 0.7 µm) and frozen immediately at −80 °C in liquid nitrogen until the analysis. Analyses were performed at the Laboratoire d'Océanographie de Villefranche (LOV). Filters were extracted in 3 mL methanol (100 %) for 2 h, disrupted by sonication, centrifuged and filtered (Whatman GF/F). The extracts were injected within 24 h onto a reversed phase C8 Zorbax Eclipse column (dimension: 3 mm × 150 mm, 3.5 µm pore size). Instrumentation comprised an Agilent Technologies 1100 series HPLC system with diode array detection at 450 nm (carotenoids and chlorophylls *c* and *b*), 676 nm (chlorophyll *a* and derivatives), and 770 nm (bacteriochlorophyll *a*). The concentrations of 21 pigments, including the chlorophyll *a* (Chl *a*), were obtained and used in this study (see Table 1 for details and pigment abbreviations). The limits of detection (3 × noise) for the different pigments, based on a filtered volume of 2 L ranged from 0.0001 to 0.0006 mg m^{-3}. The precision of the instrument was tested using injected standards and showed a variation coefficient of 0.35 %. Moreover, previous tests of the precision of the instrument and method used here were conducted on field samples replicates. A coefficient of variation of 3.2 % and 4 % was found for the primary and secondary pigment, respectively. Such precision was in accordance with the 3 % standard high precision required in the analysis of field samples (Hooker et al., 2005).

2.2 Light microscopy and flow cytometry

One to six depths were sampled in the upper 100 m of the water column for taxonomic identification and enumeration of phytoplankton cells by light microscopy. Samples were preserved in acidic Lugol's solution and stored in the dark at 4 °C until analysis. The counting of cells > 3 µm was performed using an inverted microscope (Wild Heerbrugg and Zeiss Axiovert 10) following the Utermöhl method with settling columns of 25 mL and 50 mL (Lund et al., 1958). A minimum of 400 cells were counted over at least 3 transects. Autotrophic and heterotrophic protists were counted. The autotrophic phytoplankton was shared in 10 classes plus a group of unidentified flagellates (Ta-

BGD
11, 14489–14530, 2014

ble 2). Unidentified cells (> 3 µm) represented less than 10 % of the total cell abundance over the shelf but reached 75 % of the total cell abundance over the basin. Half of the unidentified cells had a size smaller than 5 µm. Microscopic analysis, poorly suited to small-sized phytoplankton counting, was completed by enumeration of picophytoplankton (1–3 µm) by flow cytometry analysis (Marie et al., 1997) performed onboard using a FACSAria (Becton Dickinson, San Jose, CA, USA) and following the method described in Balzano et al. (2012).

2.3 Converting abundance to carbon biomass

Phytoplankton abundances obtained by light microscopy and flow cytometry were converted into carbon biomass (Table 2). The carbon biomass (C, ng C m^{-3}) is obtained by multiplying cell abundance (A, cells L^{-1}) by mean cellular carbon content (CC, ng C cell^{-1}) for each phytoplankton group:

$$C = A \times \mathrm{CC},$$

where CC was derived from cell biovolume BV (µm^3) using three conversion equations determined by regression analysis on a large dataset (Menden-Deuer and Lessard, 2000). Diatoms and dinoflagellates require particular formulas because of their low (diatoms) or high (dinoflagellates) specific carbon content relative to other protists:

Diatoms: $\mathrm{CC} = 0.288 \times \mathrm{BV}^{0.811}$

Dinoflagellates: $\mathrm{CC} = 0.760 \times \mathrm{BV}^{0.819}$

All other protists (except diatoms and dinoflagellates): $\mathrm{CC} = 0.216 \times \mathrm{BV}^{0.939}$,

where species BV were compiled from Olenina et al. (2006). When species BV were not referenced, biovolumes were estimated according to cell shape and dimensions (Bérard-Therriault et al., 1999) using appropriate geometric formulas (Olenina et al., 2006). Replicate measurments of the diameter of some common diatom and dinoflagellate species shows a variability in the biovolume around 30 % (Menden-Deuer and Lessard, 2000; Olenina et al., 2006). A 30 % overestimation of the biovolume of

BGD
11, 14489–14530, 2014

a species would cause a 20 to 30 % overestimation of its carbon biomass depending on the conversion equation used.

According to the three conversion equations, a large sized dinoflagellate (BV = 10 000 μm^3) contains 3 times more carbon than a diatom of the same biovolume and 15 % more carbon than a protist of the same biovolume. However, in the case of a small cell volume (BV = 10 μm^3), a dinoflagellate would contain 2.5 times more carbon than both a diatom and a protist.

2.4 Pigment interpretation: CHEMTAX

The CHEMTAX method (Mackey et al., 1996) was used to estimate the algal class biomass from measurements of in situ pigment. Two input are required to create the matrix ratio used to run the CHEMTAX program: the major phytoplankton groups present in our study area (chemotaxonomic classes) and their pigment content expressed as initial "pigment/TChl *a*" ratios where TChl *a* is the total Chl *a* concentration, i.e. the sum of Chl *a* and Chlide *a* (Table 3a).

The algal groups identified by microscopy were grouped in 9 chemotaxonomic classes. The very high dominance of the centric diatom *Chaetoceros socialis* in several stations over the shelf allowed to accurately define the pigment/TChl *a* ratios of the diatom class. For the other phytoplankton groups, due to their specific pigment signatures were always mixed with other group signatures, we used the pigment/TChl *a* ratios from the literature. Then, we chose the ratios representative of the dominant species associated with each chemotaxonomic class previously identified with microscopy. The dinoflagellate class represents the dinoflagellates containing peridinin as *Heterocapsa rotundata* whose ratio Peri/TChl *a* was set to 0.6 (Vidussi et al., 2004). The c_3-flagellates group corresponds to the Dino-2 class defined in Higgins et al. (2011) which included the dinoflagellates type 2 lacking pigment peridinin. We chose here to replace the group name Dino-2 by c_3-flagellates because we think the caracteristics of this groups, i.e. a relatively high Chl c_3 concentration relative to their But-fuco and Hex-fuco concentrations, included a larger diversity of flagellates including raphydo-

BGD
11, 14489–14530, 2014

phytes, dictyochophytes in addition to the autotrophic dinoflagellates lacking peridinin. The cryptophytes were detected by the presence of Allo pigment. The haptophytes type 7 class refers to the prymnesiophytes type *Chrysochromulina* spp. discriminated by a high ratio of Hex-fuco to TChl *a*. In contrast, the chrysophytes and pelagophytes contained a high ratio of But-fuco to TChl *a*. Finally, three groups of green algae containing Chl *b* were considered: the chlorophytes, the prasinophytes type 2 and the prasinophytes type 3. The prasinophytes type 3 containing the pigments Pras is representative of the pico-sized species *Micromonas* sp. while the type 2 is associated to prasinophytes lacking Pras as the nano-sized *Pyramimonas* sp. The chlorophytes were evidenced by significant concentrations of Lut, a characteristic pigment of this group (Del Campo et al., 2000). The effect of light levels on pigment ratios was taken into account by considering two matrix ratio, a high light matrix ratio run on surface samples (0–20 m) and low light matrix ratios run on subsurface samples (20–200 m). Moreover, photoprotective carotenoids (PPC = Diadino + Diato + Zea + Viola + Car) were not used since they varied strongly with irradiance and/or they are taxonomically widespread (Demers et al., 1991). Finally, we carried out independent CHEMTAX runs for shelf and basin samples to minimize the effects of the growth and nutrient conditions on the pigment interpretation.

The ratio pigment/Chl *a* for various algal taxa used as "seed" values for the CHEMTAX analysis were chosen from the literature. However, the pigment ratios for a real sample are unlikely to be known exactly due to regional variations of individual species, strain differences within a given species and local changes in algal physiology due to environmental factors such as temperature, salinity, light field, nutrient stress and mixing regimes (Mackey et al., 1996).

Therfore, to test the sensitivity of CHEMTAX, ten further high light and low light pigment ratio tables were generated by multiplying each cell of our initial matrix ratio by a randomly determined factor F, where $F = 1 + S \cdot (R - 0.5)$. S is a scaling factor (normally 0.7), and R is a random number between 0 and 1 generated using the Microsoft Excel RAND function. The random matrix ratios were created using a template pro-

BGD
11, 14489–14530, 2014

vided by Thomas Wright (CSIRO, Australia). For the shelf and basin subset, each of the ten low light and high light ratio tables were used as the starting point for a CHEMTAX optimization using iteration and a steepest descent algorithm to find a minimum residual. The solution with the smallest residual (final ratio matrix, Table 3b) was used to estimate the adundance of the phytoplankton classes, ie the part of the total Chl *a* associated to each phytoplankton class. The results of the ten matrices were used to calculate the average and standard deviation of the abundance estimates.

3 Results and discussion

3.1 Spatial distribution of accessory pigments

The distribution of TChl *a* showed large horizontal and vertical variability in the Beaufort Sea in August 2009. A subsurface chlorophyll *a* maximum (SCM) was generally present both over the shelf (35 ± 8 m) and deep waters of the Beaufort Sea (61 ± 7 m). Surface TChl *a* was twice higher on the shelf (0.20 ± 0.13 mg Chl *a* m^{-3}, Fig. 2a) than in the basins (Fig. 2c) and SCM TChl *a* was 10 times higher over the shelf (2.84 ± 2.55 mg Chl *a* m^{-3}, Fig. 2b) than in the basins (Fig. 2d). The highest chlorophyll biomasses (> 6 mg Chl *a* m^{-3}) were observed at the SCM close to the shelf break (St 260 and 780, Figs. 1 and 2b). Such high values contrast with the low ones (< 1 mg Chl *a* m^{-3}) observed during autumn in the same area in 2002 and 2003 (Brugel et al., 2009).

The concentrations of accessory pigments also varied significantly across shelf and basin stations and between the surface and the SCM. The highest biomasses, observed at the SCM of shelf waters, were associated with the dominance of Fuco and Chl $c_{1+}c_2$. These two pigments characteristic of diatoms represented 56 % and 23 % of the total accessory pigments biomass, respectively (Fig. 2b). The presence of degradation pigments of Chl *a* at the SCM of the shelf (Chlide *a* + Pheide *a* + Phe *a* = 14 % of total accessory pigments) indicated the presence of zooplankton fecal pellets or cel-

BGD
11, 14489–14530, 2014

lular senescence (Bidigare et al., 1986). The remaining 7 % were mainly associated to photoprotective carotenoids (Diadino + Diato + Zea + Viola + Car = 6.7 % of total accessory pigments).

In surface waters of the shelf (Fig. 2a), pigment assemblages were indicative of diverse communities consisting of diatoms, dinoflagellates, cryptophytes, prymnesiophytes and green algae. The contribution of Fuco (34 % of total accessory pigments), Chl $c_{1+}c_2$ (13 % of total accessory pigments) and degradation products of Chl *a* (9.7 %) decreased while the proportion of Chl *b* to total accessory pigments increased from 0.3 % at the SCM to 9 % at the surface. Peri and Allo pigments, reflecting dinoflagellates and cryptophytes, were observed at stations 394 and 680 but remained poorly represented otherwise. The high contribution of photoprotective carotenoids to total accessory pigments (16.1 %), compared to surface waters (6.7 %), indicated the response of phytoplankton to high light (Frank et al., 1994; Fujiki and Taguchi, 2002).

In the basin, pigments associated to green algae (Chl *b*, Pras, Neo, Viola, Lut) and nanoflagellates (Hex-fuco, But-fuco, Chl c_3) increased at the expense of diatom pigments, ie Fuco and Chl $c_{1+}c_2$ (Fig. 2c and d). The highest contribution of nanoflagellate pigments Hex-fuco (18 %), But-fuco (9 %) and Chl c_3 (9 %) were observed at the SCM. In contrast, the contribution of the green algal pigments Chl *b* (23 %), Viola (5.9 %) and Lut (4.3 %), was higher at the surface than at the SCM. Degradation products represented less than 3 % of the total pigment load. Like on the shelf, the contribution of photoprotective carotenoids was three to four times higher at the surface (≈ 20 %) than at the SCM (5.5 %).

The few historical pigment data available for the Canadian Arctic show spatial patterns similar to those reported here. Hill et al. (2005) in the western Beaufort Sea and Coupel et al. (2012) in the Canada Basin and the Chukchi Sea agree on the dominance of Fuco and Chl $c_{1+}c_2$ over the shelf and an increase of pigments indicative of green algae (Pras, Chl *b*) and nanoflagellates (Hex-fuco, But-fuco) offshore. However, some differences also exist, possibly reflecting the influence of distinct environmental conditions on the phytoplankton assemblage. While a higher contribution of Fuco

BGD
11, 14489–14530, 2014

was found in oligotrophic surface waters associated to strong ice melt during summer 2008 (Coupel et al., 2012), Hill et al. (2005) found a greater contribution of Pras during the relatively icy summer of 2002. Furthermore, the contribution of Pras at the SCM of basin stations was twice higher in 2008 than in 2002. Finally the pigments Hex-fuco and Chl c_3, characteristics of prymnesiophytes, contributed less in both 2002 and 2008 studies than in our 2009 data.

3.2 Phytoplankton group contribution

The surface and subsurface pigment assemblages shown in Fig. 2 were converted into relative contributions of main phytoplankton groups to TChl *a* with the CHEMTAX software. We first tested the sensitivity of the software by running CHEMTAX on our dataset using 5 different matrix ratios from previous studies of polar oceans. The resulting CHEMTAX interpretation of the pigment assemblages varies widely according to the matrix used (Fig. 3). The diatom contribution to SCM assemblages at basin stations of the Beaufort Sea varied from 3.5 % when using a parameterization for the North Polynya to 40 % when using a parameterization for the Antarctic Peninsula. Similarly, the prasinophytes contribution ranged from 15 % to 46 % depending on the initial matrix ratio used. These differences arise from the different species and pigment/TChl *a* ratios used as "seed" values in CHEMTAX. Optimizing "seed" values for our study clearly requires an investigation of dominant species and their pigment content in the Beaufort Sea. Here we did this by first identifying the dominant phytoplankton species under optical microscopy (see Sect. 2.4). Our results show that running CHEMTAX with a randomly modified version of our initial matix ratio does not significantly modify the abundance estimates of the phytoplankton classes. The standard deviation in estimating the relative abundance of the phytoplankton classes ranged between 0.1 % and 8 % with an average deviation of 2 %. Highest deviation was found for the Prasino-2 and Prasino-3 classes (about 5 %) while the variation of the others groups was less than 2 % on average.

BGD
11, 14489–14530, 2014

After running CHEMTAX on our dataset, the stations were classified with the *k*-means clustering method (MacQueen, 1967) according to their pigment ressemblance/dissemblance. Four significantly different phytoplankton communities were highlighted by the cluster classification (Fig. 4a). Cluster 1 was dominated at 95 % by diatoms and represented the SCM of stations located on the shelf as well as surface waters close to Cap Bathurst and the Mackenzie estuary (Fig. 4b and c). Cluster 2 included surface waters of basin and shelf stations, characterized by a dominance of green algae (40 %) shared between type 3 prasinophytes (25 %) and chlorophytes (16 %). Diatoms, dinoflagellates and cryptophytes were also major contributors of cluster 2 with 20 %, 12 % and 7 % respectively. Clusters 3 and 4 were restricted to the SCM of basin stations and characterized by a high contribution of flagellates (Fig. 4a and c). Cluster 4 was dominated by prymnesiophytes (41 %) while c_3-flagellates dominated the cluster 3 (28 %). The contribution of green algae remained high in clusters 3 and 4 but was shared between prasinophytes of types 2 and 3 while chlorophytes were not longer present.

3.3 Linkages between phytoplankton assemblages and environmental factors

The four assemblages of phytoplankton inferred from pigments (Fig. 4a) were compared to environmental conditions (Table 4). The green algae, especially pico-sized prasinophytes of type 3, dominated the oligotrophic (0.12 ± 0.13 mg Chl $a\,m^{-3}$) and nutrient-depleted surface waters (Cluster 2). It is consistant with the high surface/volume ratios of the picophytoplankton, which allows for more effective nutrient acquisition and better resistance to sinking. Dominance of the prasinophyte *Micromonas* sp. in the Beaufort Sea has been previously highlighted and was shown to be more pronounced under reduced sea ice cover (Comeau et al., 2011; Li et al., 2009; Lovejoy et al., 2007). Otherwise, the high Lut/Chl *b* ratio (≈ 0.2) points to a significant contribution of chlorophytes in surface waters. The Mackenzie River could have spread this freshwater group in the Beaufort Sea (Brugel et al., 2009) as supported by the restriction to the surface fresh waters of the chlorophytes. The dinoflagellates observed

BGD
11, 14489–14530, 2014

in surface waters have been previously underlines as a major contributor of the large autotrophic cells abundance on the Mackenzie shelf (Brugel et al., 2009).

At the SCM of shelf stations (Cluster 1), nitrate concentrations were high ($3.1 \pm 2.8\,\mu mol\,L^{-1}$, Table 4) and possibly support substantial new production. The highest biomasses of the cruise ($1.8 \pm 2.3\,mg\,Chl\,a\,m^{-3}$ and $80 \pm 45\,mg\,C\,m^{-3}$) were measured in these waters and were related to a high dominance of diatoms. The diatom population could be fed by a cross-shelf flow of nitrate-rich waters from the basin to the shelf bottom (Carmack et al., 2004; Forest et al., 2013). The optical microscopy showed a strong dominance of the colonial centric diatoms *Chaetoceros socialis* ($\approx 1 \times 10^6\,cell\,L^{-1}$, data not shown). This species is relatively small ($\approx 10\,\mu m$) and often observed in succession to larger ones such as *Thalassiosira* spp. or *Fragilariopsis* spp. when the ice-free season advances (Booth et al., 2002; Vidussi et al., 2004; von Quillfeldt, 2000). Diatoms also dominated surface waters north of Cape Bathurst and near the Mackenzie estuary but their biomass was lower and related to different species according to microscopy (i.e. *Thalasiossira nordenskioeldii* and *Pseudo-nitzschia* sp.). Sporadic high concentration of Chl *a* and occurrence of *Chaetoceros socialis* was previously observed in September 2005 at the SCM and at the surface following local upwelling events and advective input of nutrients from the deep basin (Comeau et al., 2011).

The SCM of basin stations was dominated by two distinct flagellate assemblages, which are distinguished by their Hex-fuco/But-fuco ratio. The prymnesiophytes characterized by a high Hex-fuco/But-fuco ratio (≈ 3) dominated cluster 4 while c_3-flagellates associated to a low Hex-fuco/But-fuco ratio (≈ 1) dominated cluster 3. The shift in assemblages was related to the vertical position of the SCM relative to the nitracline. The prymnesiophytes, mainly associated to *Chrysochromulina* sp., dominated when the SCM matched the nitracline, whereas c_3-flagellates dominated when the SCM was below the nitracline (Fig. 5). Incidentally, the relatively shallow prymnesiophyte-dominated SCM ($\approx 55\,m$) was exposed to more light ($PAR = 4.7 \pm 1.7\,\mu M\,m^{-2}\,s^{-1}$, Table 4) but less nitrate ($0.5 \pm 0.2\,\mu mol\,L^{-1}$, Table 4) than the deeper c_3-flagellate-dominated SCM ($\approx 65\,m$) that occurred at a PAR of $2.2 \pm 1.2\,\mu M\,m^{-2}\,s^{-1}$ and 10-fold higher nitrate

BGD
11, 14489–14530, 2014

concentrations ($5.1 \pm 2.7\,\mu mol\,L^{-1}$). We stated that the c_3-flagellate group was comprised primarily of raphidophytes. Indeed, microscopy showed that raphidophytes were present only at the SCM of basin stations, where they represented 25 % of phytoplankton carbon biomass (Table 2). The lack of photoprotective pigments in raphidophytes could explain why this group is restricted to deep SCM (Van den Hoek, 1995). A recent study based on molecular approaches showed an increase of prymnesiophytes type *Chrysochromulina* sp. since 2007 in the Beaufort Sea (Comeau et al., 2011). The prevalence of flagellates was attributed to the gradual freshening of the Beaufort Sea and increasing stratification. The lack of mixing may act to force the SCM deeper resulting in lower ambient PAR (McLaughlin and Carmack, 2010). Dominance of nanoflagellates has been previously noticed in SCM waters of the Canada Basin in conditions of intense freshwater accumulation (Coupel et al., 2012).

3.4 Cell abundance and carbon biomass: implications for carbon export

The chemotaxonomic interpretation of pigments remains semi-quantitative. CHEMTAX provide the percentage contribution of phytoplankton groups according to their relative contribution to TChl *a*. This information is relevant to monitor changes in the phytoplankton communities or any environmental changes susceptible to affect the pigment composition of plankton. A change in the relative contribution of pigments is a clear footprint of change in the structure or in the acclimation of phytoplankton communities. Nevertheless, to investigate the implications of phytoplankton changes on food webs and the biological pump, the pigment data must be converted into contribution to total abundance or carbon biomass. However, this conversion is not always straightforward since pigment chemotaxonomy and microscopy measure different parameters with different units (i.e. cell numbers, $mg\,C\,m^{-3}$ vs. $mg\,Chl\,a\,m^{-3}$).

Not surprisingly, the contribution of different phytoplankton groups to total cell abundance differed from their contribution to total phytoplankton carbon biomass. The picophytoplankton largely dominated cell abundance, except on the shelf where di-

BGD
11, 14489–14530, 2014

atoms dominated the SCM (Fig. 6, Table 2), but contributed only 0–3 % and 6–7 % of the total phytoplankton carbon biomass over the shelf and basin, respectively. Phytoplankton larger than 3 µm dominated carbon biomass at all stations (Fig. 7, Table 2). The minimum total phytoplankton abundance was observed at SCM of the basin (2500 ± 2500 cell mL^{-1}) and the maximum in surface of the shelf (4400 ± 1400 cell mL^{-1}). Nevertheless, the total phytoplankton abundance over the shelf was not significantly higher than in the Beaufort basin. Conversely, average carbon biomass at the surface was 3 times higher on the shelf (64 ± 22 mg C m^{-3}) than in the basin (25 ± 7 mg C m^{-3}). The difference was more pronounced at the SCM, where carbon biomass was 8 times higher at shelf stations (110 ± 57 mg C m^{-3}) than at basin stations (14 ± 5 mg C m^{-3}). This contrast was attributed to the dominance of SCM carbon biomass (up to 90 %) by diatoms on the shelf. Otherwise the carbon biomass was dominated at 50–75 % by dinoflagellates, which represented less than 15 % of total cell abundance (Table 2). The highest biomasses of dinoflagellates occurred in surface waters of the Mackenzie canyon area (Stations 600's, Fig. 3a and c) and were associated with high biomasses of other heterotrophs, mainly ciliates. Raphidophytes also made a substantial contribution (26 %) to the total phytoplankton carbon biomass at the SCM of basin stations.

Since the estimated contributions of phytoplankton groups to carbon biomass differ from contributions to cell abundance one might ask which of the two variables should be reflected by the chemotaxonomic approach. Overall, the contribution of algal groups to TChl *a* (CHEMTAX) showed better agreement with their contribution to total cell abundance (Fig. 9) than to total carbon biomass (Fig. 8). The best agreement between CHEMTAX and relative abundance and biomass was obtained for diatoms (Figs. 8a and 9a). For nanoflagellates and picophytoplankton, CHEMTAX showed a moderate correlation with relative abundance (Fig. 8b and c) and a weak one with relative biomass (Fig. 9b and c). In fact, CHEMTAX underestimates the importance of picophytoplankton and nanoflagellates in terms of cell abundance but overestimates their importance in terms of carbon biomass, as shown by the position of data points with respect to the 1:1 line in Figs. 8b and c and 9b and c. We observed that the contri-

BGD
11, 14489–14530, 2014

bution of picophytoplankton to TChl *a* became significant only when its contribution to total cell abundance exceeded 80 % (Fig. 8b). Obviously, the underestimation of small phytoplankton abundance by chemotaxonomy is explained by the lower amount of pigment including Chl *a* in small cells compared to large cells. On the other hand, the ratio of carbon to TChl *a* (C/TChl *a*) in phytoplankton increases with cell volume (Geider et al., 1986). The fact that small cells are richer in Chl *a* than large cells for a similar carbon biomass could explain the overestimation in the contribution of small phytoplankton to total carbon biomass by the chemotaxonomy. Based on the relationships between cell volume and content in Chl *a* and carbon proposed by Montagnes et al. (1994), we calculate the ratio C/TChl *a* of a *Micromonas* sp. (1 μm^3) to be twice lower than in diatoms or dinoflagellates (1000 μm^3). Indeed, the pigments are mainly in the periphery of the cell, which means that the intracellular pigment density increases as the surface area to volume ratio increases. This is clearly demonstrated by comparing the mean C/TChl *a* ratio of the surface waters dominated by diatoms (Cluster 1 surf: C/TChl $a = 280 \pm 150$, Table 4), with the surface waters dominated by *Micromonas* sp. (Cluster 2, C/TChl $a = 160 \pm 110$). The weaker relation between CHEMTAX and carbon biomass could have been induced by these variations in the C/TChl *a* ratios of the phytoplankton and by the different transfer equations used to determine the carbon biomass from the biovolume (see Sect. 2.3).

No significant correlation was observed between CHEMTAX and microscopy for dinoflagellates, prymnesiophytes, chrysophytes, chlorophytes and cryptophytes. Such inconsistences are mainly attributed to the low accuracy of visual counts for nano-sized flagellates. Up to 35 % of the visible flagellates were categorized as unidentified and others may have been overlooked because of poor conservation. The most surprising divergence between CHEMTAX and microscopy occurred for dinoflagellates (Figs. 8d, 9d). Despite the high contribution of this group to carbon biomass (Fig. 7), it rarely contributed more than 10 % of the TChl *a* according to CHEMTAX. While such a discrepency may generally arise from the large biovolume and high C/TChl *a* ratio of dinoflagellates compared to other groups, in our study it was presumably caused

BGD
11, 14489–14530, 2014

by the inability of CHEMTAX to detect dinoflagellates of the genera *Gymnodinium* sp. and *Gyrodinium* sp., which lack Peri (Jeffrey et al., 1997). Indeed, we found no correlation between dinoflagellate abundance and the unambiguous pigment Peri used by CHEMTAX to detect this group (r^2 = 0.04, not shown). Only the surface waters of the stations 394 and 680 dominated by an autotrophic dinoflagellate (*Heterocapsa rotundata*) known to possess a relative high Peri content showed the presence of Peri in relative high proportion. Molecular analyses indicated that the nonphotosynthetic heterotrophic species *Gyrodinium rubrum* dominated the dinoflagallate assemblages in the region (D. Onda, personal communication, 2014). Heterotrophic dinoflagellates would only contain diagnostic pigments if they ingested it with their prey. It is known that heterotrophic and mixotrophic dinoflagellates feed on diverse prey items including bacteria, picoeukaryotes, nanoflagellates, diatoms, other dinoflagellates, heterotrophic protists, and metazoans due to their diverse feeding mechanisms (Jeong et al., 2010) and are likely to be a significant consumers of bloom-forming diatoms (Sherr and Sherr, 2007). It follows that the presence of heterotrophic dinoflagellates could potentially lead to overestimation of the phytoplanktonic groups they ingest when looking at the pigment concentrations. In contrast to the study of (Brugel et al., 2009) in the Beaufort Sea during summer 2002, when autotrophic dinoflagellates contributed as much as heterotrophic dinoflagellates abundance, heterotrophic dinoflagellates were largely dominant in 2009. Strict autotrophic dinoflagellates represented only 13 % of total dinoflagellate biomass.

The high contribution of heterotrophic dinoflagellates and ciliates in surface waters suggest an important transfer of organic material to the pelagic food web and a reduced sinking export of high quality algal material, due to assimilation and remineralization as mentioned by Juul-Pedersen et al. (2010). This scenario also agrees with the observation of Forest et al. (2013) showing a limited vertical exchange of nutrients and carbon between the surface and sub-surface and the establishment of a food web exclusively based on small protists using recycled nutrients. Conversely, the high abundance of centric diatoms at the SCM on the shelf could lead to an effective transfer of high qual-

BGD
11, 14489–14530, 2014

ity algal material to the benthos as evidenced by the very large pool and fluxes of POC observed at shelf stations by Forest et al. (2013) during the same cruise. The high abundance of Fuco previously observed in the sediment of the Mackenzie shelf during summer supports the hypothesis of an efficient export of diatoms to the seafloor (Morata et al., 2008).

4 Conclusions

We evaluated the utility of CHEMTAX to characterize phytoplankton dynamics in the Beaufort Sea in late summer 2009. Based on the taxonomic information from optical microscopy, a matrix ratio was created specifically for the Beaufort Sea and run using the CHEMTAX software.

The interpretation of the pigment data by CHEMTAX highlights linkages between the phytoplankton distribution and environmental parameters commonly observed in Arctic Ocean. The productive and nutrient rich sub-surface waters of the shelf were dominated (95 % of abundance) by the centric diatom identified by microscopy as *Chaetoceros socialis*. In contrast, oligotrophic, nutrient-depleted surface waters over the shelf and basin presented the highest contribution of green algae (48 % of the TChl *a*), dominated by the pico-prasinophytes *Micromonas* sp.

The use of pigments and CHEMTAX also revealed more subtle information difficult to observe with other taxonomic methods. Indeed, two populations of flagellates were highlighted in sub-surface waters of the basin: prymnesiophytes, rich in Hex-Fuco pigment, and a group of various flagellates rich in Chl c_3 and Fuco (i.e. c_3-flagellates). The prymnesiophytes dominated where the sub-surface chlorophyll maximum was located above 60 m and were associated with higher light availability and lower nutrient concentrations. In contrast, the c_3-flagellates dominated when the sub-surface chlorophyll maximum was deeper than 60 m and the organisms were exposed to higher nitrate concentrations and lower light availability. Flagellate populations that are able to grow at deep sub-surface chlorophyll *a* maximum should be closely monitored in a context

BGD
11, 14489–14530, 2014

of a deepening of the nutricline observed since a decade in the Canadian Arctic due to increased surface freshening and stratification.

The present study underlines the high sensitivity of CHEMTAX to the initial matrix ratio chosen and the misinterpretation induced by a blind use of a matrix ratio calibrated in regions other than the targeted one. Therefore, we recommend that future pigment studies in the Beaufort Sea use the CHEMTAX parameterization developed in the present work.

However, some issues and inconsistences should be considered when using CHEMTAX in the Beaufort Sea and, probably, in the entire Arctic Ocean. Despite high biomasses, the heterotrophic dinoflagellates of the Gymnodinium/Gyrodinium complex were undetected by pigment analyses since they lack peridinin. High heterotrophy can lead to misinterpretation because CHEMTAX potentially takes into account other pigments present in the algae ingested by dinoflagellates. Additionally, CHEMTAX underestimates the importance of small phytoplankton in terms of cell abundance but overestimates their importance in terms of carbon biomass. The variability in pigment content per cell and in the C/TChl *a* ratio makes it difficult to relate pigment signatures to carbon biomass or cell abundance. The contribution of small phytoplankton to TChl *a* was 2 to 3 times higher than their contribution to carbon biomass due to generally low C/TChl *a* ratios of these organisms. The opposite was observed for large phytoplankton like dinoflagellates for which contribution to total biomass was higher than their contribution to TChl *a*. Overall, we found the contribution of algal groups to TChl *a* (CHEMTAX) showed better agreement with their contribution to total cell abundance than their contribution to the total phytoplankton carbon biomass.

In contrast, for localized use of CHEMTAX, as presented in our study, the large pigment dataset in Arctic Ocean could be used to determine averaged pigment ratios for the dominant Arctic phytoplankton groups and create a single pan-Arctic matrix ratio for CHEMTAX. With this goal in mind, we advise creating a simple matrix ratio in CHEMTAX to retrieve the three functional groups diatoms, nanoflagellates and picophytoplankton successfully validated by optical microscopy. Indeed, a weak or no

BGD
11, 14489–14530, 2014

correlation was found between CHEMTAX and microscopy for the other groups: chrysophytes, prymnesiophytes, chlorophytes and cryptophytes. Nonetheless, we attribute these dissimilarities to the high proportion of flagellates that are unidentified or overlooked by microscopy rather than a misinterpretation by CHEMTAX.

Alternatively, when taxonomic information is lacking in the targeted study area, we recommend using the raw pigment data and selecting key pigment ratios rather than the blind use of CHEMTAX. The high reproducibility of the HPLC method to measure pigment concentrations insures a robust approach for detecting seasonal or interannual changes in phytoplankton communities when the others methods lack accuracy.

Acknowledgements. This study was conducted as part of the Malina Scientific Program led by Marcel Babin and funded by ANR (Agence nationale de la recherche), INSU-CNRS (Institut national des sciences de l'Univers – Centre national de la recherche scientifique), CNES (Centre national d'études spatiales) and ESA (European Space Agency). The present study started at the LOCEAN laboratory (UPMC – University Pierre et Marie Curie) supported by the Arctic Tipping Point project (ATP, http://www.eu-atp.org) funded by FP7 of the European Union (contract #226248) and was continued at Laval University (Quebec, Canada) funded by the Canada Excellence Research Chair in "Remote sensing of Canada's new Arctic frontier" and Québec-Océan. We are grateful to the crew and captain of the Canadian research icebreaker CCGS *Amundsen*. Thanks to S. Lessard for the phytoplankton identification and enumeration by light microscopy and to J.Ras for pigment analyses.

References

Alou-Font, E., Mundy, C. J., Roy, S., Gosselin, M., and Agustí, S.: Snow cover affects ice algal pigment composition in the coastal Arctic Ocean during spring, Mar. Ecol.-Prog. Ser., 474, 89–104, 2013.

Alvain, S., Moulin, C., Dandonneau, Y., and Breon, F. M.: Remote sensing of phytoplankton groups in case 1 waters from global SeaWiFS imagery, Deep-Sea Res. Pt. I, 52, 1989–2004, 2005.

BGD
11, 14489–14530, 2014

Ansotegui, A., Trigueros, J., and Orive, E.: The use of pigment signatures to assess phytoplankton assemblage structure in estuarine waters, Estuar. Coast. Shelf. S., 52, 689–703, 2001.
Balzano, S., Marie, D., Gourvil, P., and Vaulot, D.: Composition of the summer photosynthetic pico and nanoplankton communities in the Beaufort Sea assessed by T-RFLP and sequences of the 18S rRNA gene from flow cytometry sorted samples, ISME J., 6, 1480–1498, 2012.
Bérard-Therriault, L., Poulin, M., and Bossé, L.: Guide d'identification du phytoplancton marin de l'estuaire et du golfe du Saint-Laurent: incluant également certains protozoaires, Publ. spéc. can. sci. halieut. aquat., 1999.
Bidigare, R. R., Frank, T. J., Zastrow, C., and Brooks, J. M.: The distribution of algal chlorophylls and their degradation products in the Southern Ocean, Deep-Sea. Res., 33, 923–937, 1986.
Booth, B. C., Larouche, P., Bélanger, S., Klein, B., Amiel, D., and Mei, Z. P.: Dynamics of Chaetoceros socialis blooms in the North Water, Deep-Sea. Res. Pt. II, 49, 5003–5025, 2002.
Brugel, S., Nozais, C., Poulin, M., Tremblay, J. E., Miller, L. A., Simpson, K. G., Gratton, Y., and Demers, S.: Phytoplankton biomass and production in the southeastern Beaufort Sea in autumn 2002 and 2003, Mar. Ecol.-Prog. Ser., 377, 63–77, 2009.
Carmack, E. and Wassmann, P.: Food webs and physical–biological coupling on pan-Arctic shelves: unifying concepts and comprehensive perspectives, Prog. Oceanogr., 71, 446–477, 2006.
Carmack, E. C., Macdonald, R. W., and Jasper, S.: Phytoplankton productivity on the Canadian Shelf of the Beaufort Sea, Mar. Ecol.-Prog. Ser., 277, 37–50, 2004.
Comeau, A. M., Li, W. K., Tremblay, J. E., Carmack, E. C., and Lovejoy, C.: Arctic Ocean microbial community structure before and after the 2007 record sea ice minimum, PLoS ONE, 6, e27492, doi:10.1371/journal.pone.0027492, 2011.
Comiso, J. C., Parkinson, C. L., Gersten, R., and Stock, L.: Accelerated decline in the Arctic sea ice cover, Geophys. Res. Lett., 35, L01703, doi:10.1029/2007GL031972, 2008.
Coupel, P., Jin, H. Y., Joo, M., Horner, R., Bouvet, H. A., Sicre, M. A., Gascard, J. C., Chen, J. F., Garçon, V., and Ruiz-Pino, D.: Phytoplankton distribution in unusually low sea ice cover over the Pacific Arctic, Biogeosciences, 9, 4835–4850, doi:10.5194/bg-9-4835-2012, 2012.
Del Campo, J. A., Moreno, J., Rodriguez, H., Vargas, M. A., Rivas, J., and Guerrero, M. G.: Carotenoid content of chlorophycean microalgae: factors determining lutein accumulation in *Muriellopsis* sp. (Chlorophyta), J. Biotechnol., 76, 51–59, 2000.

BGD
11, 14489–14530, 2014

Demers, S., Roy, S., Gagnon, R., and Vignault, C.: Rapid light-induced-changes in cell fluorescence and in xanthophyll-cycle pigments of Alexandrium-Excavatum (*dinophyceae*) and *thalassiosira-pseudonana* (*bacillariophyceae*) – a photo-protection mechanism, Mar. Ecol.-Prog. Ser., 76, 185–193, 1991.

Falkowski, P.: The global carbon cycle: a test of our knowledge of earth as a system, Science, 290, 291–296, 2000.

Forest, A., Coupel, P., Else, B., Nahavandian, S., Lansard, B., Raimbault, P., Papakyriakou, T., Gratton, Y., Fortier, L., Tremblay, J.-É., and Babin, M.: Synoptic evaluation of carbon cycling in Beaufort Sea during summer: contrasting river inputs, ecosystem metabolism and air-sea CO_2 fluxes, Biogeosciences, 11, 2827–2856, doi:10.5194/bg-11-2827-2014, 2014.

Frank, H. A., Cua, A., Chynwat, V., Young, A., Gosztola, D., and Wasielewski, M. R.: Photophysics of the carotenoids associated with the xanthophyll cycle in photosynthesis, Photosynth. Res., 41, 389–395, 1994.

Fujiki, T. and Taguchi, S.: Variability in chlorophyll a specific absorption coefficient in marine phytoplankton as a function of cell size and irradiance, J. Plankton Res., 24, 859–874, 2002.

Geider, R., Platt, T., and Raven, J. A.: Size dependence of growth and photosynthesis in diatoms: a synthesis, Mar. Ecol.-Prog. Ser, 30, 93–104, 1986.

Grebmeier, J. M., Moore, S. E., Overland, J. E., Frey, K. E., and Gradinger, R.: Biological response to recent Pacific Arctic Sea ice retreats, Eos Trans. AGU, 91, 161–168, 2010.

Higgins, H. W., Wright, S. W., and Schlüter, L.: Quantitative interpretation of chemotaxonomic pigment data, in: Phytoplankton Pigments: Characterization, Chemotaxonomy and Applications in Oceanography, Cambridge University Press, edited by Roy, S., Llewellyn, C. A., Egeland, E, .S and Johnsen, G., United Kingdom, 257–313, ISBN 9780511732263, 2011.

Hill, V., Cota, G., and Stockwell, D.: Spring and summer phytoplankton communities in the Chukchi and Eastern Beaufort Seas, Deep-Sea Res. Pt. II, 52, 3369–3385, 2005.

Hirata, T., Hardman-Mountford, N. J., Brewin, R. J. W., Aiken, J., Barlow, R., Suzuki, K., Isada, T., Howell, E., Hashioka, T., Noguchi-Aita, M., and Yamanaka, Y.: Synoptic relationships between surface Chlorophyll-*a* and diagnostic pigments specific to phytoplankton functional types, Biogeosciences, 8, 311–327, doi:10.5194/bg-8-311-2011, 2011.

Hooker, S. B., Van Heukelem, L., Thomas, C. S., Claustre, H., Ras, J., Barlow, R., Sessions, H., Schlüter, L., Perl, J., and Trees, C.: Second SeaWiFS HPLC Analysis Round-robin Experiment (SeaHARRE-2), National Aeronautics and Space Administration, Goddard Space Flight Center, 2005.

BGD
11, 14489–14530, 2014

Hunt Jr, G. L., Stabeno, P., Walters, G., Sinclair, E., Brodeur, R. D., Napp, J. M., and Bond, N. A.: Climate change and control of the southeastern Bering Sea pelagic ecosystem, Deep-Sea Res. Pt. II, 49, 5821–5853, 2002.

Irigoien, X., Meyer, B., Harris, R., and Harbour, D.: Using HPLC pigment analysis to investigate phytoplankton taxonomy: the importance of knowing your species, Helgoland Mar. Res., 58, 77–82, 2004.

Jeffrey, S. W., Mantoura, R. F. C., and Wright, S. W.: Phytoplankton pigments in oceanography, Monographs on oceanographic methods, UNESCO, Paris, 1997.

Jeong, H., Yoo, Y., Kim, J., Seong, K., Kang, N., and Kim, T.: Growth, feeding and ecological roles of the mixotrophic and heterotrophic dinoflagellates in marine planktonic food webs, Ocean Sci. J., 45, 65–91, 2010.

Juul-Pedersen, T., Michel, C., and Gosselin, M.: Sinking export of particulate organic material from the euphotic zone in the eastern Beaufort Sea, Mar. Ecol.-Prog. Ser., 410, 55–70, 2010.

Kozlowski, W. A., Deutschman, D., Garibotti, I., Trees, C., and Vernet, M.: An evaluation of the application of CHEMTAX to Antarctic coastal pigment data, Deep-Sea Res. Pt. I, 58, 350–364, 2011.

Lewitus, A. J., White, D. L., Tymowski, R. G., Geesey, M. E., Hymel, S. N., and Noble, P. A.: Adapting the CHEMTAX method for assessing phytoplankton taxonomic composition in southeastern US estuaries, Estuaries, 28, 160–172, 2005.

Li, W. K., McLaughlin, F. A., Lovejoy, C., and Carmack, E. C.: Smallest algae thrive as the Arctic Ocean freshens, Science, 326, 539, 2009.

Lovejoy, C., Vincent, W. F., Bonilla, S., Roy, S., Martineau, M.-J., Terrado, R., Potvin, M., Massana, R., and Pedrós-Alió, C.: Distribution, phylogeny, and growth of cold-adapted picoprasinophytes in Arctic seas, J. Phycol., 43, 78–89, 2007.

Lund, J. W. G., Kipling, C., and Cren, E. D.: The inverted microscope method of estimating algal numbers and the statistical basis of estimations by counting, Hydrobiologia, 11, 143–170, 1958.

Mackey, M. D., Mackey, D. J., Higgins, H. W., and Wright, S. W.: CHEMTAX – a program for estimating class abundances from chemical markers: application to HPLC measurements of phytoplankton, Mar. Ecol.-Prog. Ser., 144, 265–283, 1996.

MacQueen, J.: Some methods for classification and analysis of multivariate observations, 1967, 14.

BGD
11, 14489–14530, 2014

Marie, D., Partensky, F., Jacquet, S., and Vaulot, D.: Enumeration and cell cycle analysis of natural populations of marine picoplankton by flow cytometry using the nucleic acid stain SYBR Green I, Appl. Environ. Microb., 63, 186–193, 1997.

McLaughlin, F. A. and Carmack, E. C.: Deepening of the nutricline and chlorophyll maximum in the Canada Basin interior, 2003–2009, Geophys. Res. Lett., 37, L24602, doi:10.1029/2010GL045459, 2010.

Menden-Deuer, S. and Lessard, E. J.: Carbon to volume relationships for dinoflagellates, diatoms, and other protist plankton, American Society of Limnology and Oceanography, Waco, Texas, USA, 2000.

Montagnes, D. J., Berges, J. A., Harrison, P. J., and Taylor, F.: Estimating carbon, nitrogen, protein, and chlorophyll *a* from volume in marine phytoplankton, Limnol. Oceanogr., 39, 1044–1060, 1994.

Morata, N., Renaud, P. E., Brugel, S., Hobson, K. A., and Johnson, B. J.: Spatial and seasonal variations in the pelagic–benthic coupling of the southeastern Beaufort Sea revealed by sedimentary biomarkers, Mar. Ecol.-Prog. Ser., 371, 47–63, 2008.

Not, F., Ramon, M., Latasa, M., Marie, D., Colson, C., Eikrem, W., Pedrós-Alió, C., Vaulot, D., and Simon, N.: Late Summer Community Composition and Abundance of Photosynthetic Picoeukaryotes in Norwegian and Barents Seas, Limnol. Oceanogr., 50, 1677–1686, 2005.

Olenina, I., Hajdu, S., Edler, L., Andersson, A., Wasmund, N., Busch, S., Göbel, J., Gromisz, S., Huseby, S., Huttunen, M., Jaanus, A., Kokkonen, P., Ledaine, I., and Niemkiewicz, E.: Biovolumes and size-classes of phytoplankton in the Baltic Sea, Baltic Marine Environment Protection Commission – HELCOM, Helsinki, 2006.

Pickart, R. S., Schulze, L. M., Moore, G. W. K., Charette, M. A., Arrigo, K. R., van Dijken, G., and Danielson, S. L.: Long-term trends of upwelling and impacts on primary productivity in the Alaskan Beaufort Sea, Deep-Sea Res. Pt. I, 79, 106–121, 2013.

Poulin, M., Daugbjerg, N., Gradinger, R., Ilyash, L., Ratkova, T., and Quillfeldt, C.: The pan-Arctic biodiversity of marine pelagic and sea-ice unicellular eukaryotes: a first-attempt assessment, Mar. Biodiv., 41, 13–28, 2010.

Riegman, R. and Kraay, G. W.: Phytoplankton community structure derived from HPLC analysis of pigments in the Faroe-Shetland Channel during summer 1999: the distribution of taxonomic groups in relation to physical/chemical conditions in the photic zone, J. Plankton Res., 23, 191–205, 2001.

BGD
11, 14489–14530, 2014

Rodriguez, F., Varela, M., and Zapata, M.: Phytoplankton assemblages in the Gerlache and Bransfield Straits (Antarctic Peninsula) determined by light microscopy and CHEMTAX analysis of HPLC pigment data, Deep-Sea. Res. Pt. II, 49, 723–747, 2002.
Rothrock, D. A., Yu, Y., and Maykut, G. A.: Thinning of the Arctic sea-ice cover, Geophys. Res. Lett., 26, 3469–3472, 1999.
Roy, S., Chanut, J.-P., Gosselin, M., and Sime-Ngando, T.: Characterization of phytoplankton communities in the lower St. Lawrence Estuary using HPLC-detected pigments and cell microscopy, Mar. Ecol.-Prog. Ser., 142, 55–73, 1996.
Sathyendranath, S., Watts, L., Devred, E., Platt, T., Caverhill, C., and Maass, H.: Discrimination of diatoms from other phytoplankton using ocean-colour data, Mar. Ecol.-Prog. Ser., 272, 59–68, 2004.
Schlüter, L., Møhlenberg, F., Havskum, H., and Larsen, S.: The use of phytoplankton pigments for identifying and quantifying phytoplankton groups in coastal areas: testing the influence of light and nutrients on pigment/chlorophyll a ratios, Mar. Ecol.-Prog. Ser., 192, 49–63, 2000.
Sherr, E. B. and Sherr, B. F.: Heterotrophic dinoflagellates: a significant component of microzooplankton biomass and major grazers of diatoms in the sea, Mar. Ecol.-Prog. Ser., 352, 187–197, doi:10.3354/meps07161, 2007.
Sigman, D. M. and Boyle, E. A.: Glacial/interglacial variations in atmospheric carbon dioxide, Nature, 407, 859–869, 2000.
Stroeve, J. C., Serreze, M. C., Holland, M. M., Kay, J. E., Malanik, J., and Barrett, A. P.: The Arctic's rapidly shrinking sea ice cover: a research synthesis, Climatic Change, 110, 1005–1027, 2011.
Suzuki, K., Minami, C., Liu, H., and Saino, T.: Temporal and spatial patterns of chemotaxonomic algal pigments in the subarctic Pacific and the Bering Sea during the early summer of 1999, Deep-Sea. Res. Pt. II, 49, 5685–5704, 2002.
Taylor, R. L., Semeniuk, D. M., Payne, C. D., Zhou, J., Tremblay, J.-É., Cullen, J. T., and Maldonado, M. T.: Colimitation by light, nitrate, and iron in the Beaufort Sea in late summer, J. Geophys. Res.-Oceans, 118, 3260–3277, 2013.
Tremblay, J. E., Belanger, S., Barber, D. G., Asplin, M., Martin, J., Darnis, G., Fortier, L., Gratton, Y., Link, H., Archambault, P., Sallon, A., Michel, C., Williams, W. J., Philippe, B., and Gosselin, M.: Climate forcing multiplies biological productivity in the coastal Arctic Ocean, Geophys. Res. Lett., 38, L18604, doi:10.1029/2011GL048825, 2011.

BGD
11, 14489–14530, 2014

Uitz, J., Claustre, H., Morel, A., and Hooker, S. B.: Vertical distribution of phytoplankton communities in open ocean: an assessment based on surface chlorophyll, J. Geophys. Res., 111, doi:10.1029/2005JC003207, 2006.
Van den Hoek, C.: Algae: an introduction to phycology, Cambridge University Press, 1995.
Van Heukelem, L. and Thomas, C. S.: Computer-assisted high-performance liquid chromatography method development with applications to the isolation and analysis of phytoplankton pigments, J. Chromatogr. A, 910, 31–49, 2001.
Vidussi, F., Roy, S., Lovejoy, C., Gammelgaard, M., Thomsen, H., Booth, B., Tremblay, J. E., and Mostajir, B.: Spatial and temporal variability of the phytoplankton community structure in the North Water Polynya, investigated using pigment biomarkers, Can. J. Fish. Aquat. Sci., 61, 2038–2052, 2004.
von Quillfeldt, C. H.: Common Diatom Species in Arctic Spring Blooms: Their Distribution and Abundance, Bot. Mar., 46, 499–516, doi:10.1515/BOT.2000.050, 2000.
Wassmann, P. and Reigstad, M.: Future arctic ocean seasonal ice zones and implications for pelagic-benthic coupling, Oceanography, 24, 220–231, 2011.
Wassmann, P., Duarte, C. M., Agusti, S., and Sejr, M. K.: Footprints of climate change in the Arctic marine ecosystem, Glob. Change. Biol., 17, 1235–1249, 2011.
Wright, S. W. and Jeffrey, S. W.: Pigment Markers for Phytoplankton Production, in: Marine Organic Matter: Biomarkers, Isotopes and DNA, Volkman, J. (Ed.), The Handbook of Environmental Chemistry, Springer Berlin Heidelberg, 2006.
Wright, S. W., Thomas, D. P., Marchant, H. J., Higgins, H. W., Mackey, M. D., and Mackey, D. J.: Analysis of phytoplankton of the Australian sector of the Southern Ocean: comparisons of microscopy and size frequency data with interpretations of pigment HPLC data using the "CHEMTAX" matrix factorisation program, Mar. Ecol.-Prog. Ser., 144, 285–298, 1996.

BGD
11, 14489–14530, 2014

Table 1. Distribution of major taxonomically significant pigments in algal classes using SCOR abbreviations (Jeffrey et al., 1997).

Pigment	Abbreviation	Specificity
Chlorophylls		
Chlorophyll *a*	Chl *a*	All photosynthetic algae
Bacteriochlorophyll *a*	BChl *a*	Photosynthetic bacteria
Chlorophyll *b*	Chl *b*	Dominant in green algae
Chlorophyll $c_1 + c_2$	Chl $c_1 + c_2$	Minor in red algae
Chlorophyll c_3	Chl c_3	Dominant in haptophyte, many diatoms and some dinoflagellates
Chlorophyllide *a*	Chlide *a*	Degradation products of chlorophyll *a*
Pheophorbide *a*	Pheide *a*	Degradation products of chlorophyll *a*
Pheophytin *a*	Phe *a*	Degradation products of chlorophyll *a*
Carotene(s)	Car	Dominant in chlorophytes, prasinophytes, minor in all other algal groups
Xanthophylls		
Alloxanthin	Allo	Major in Cryptophytes
19'-butanoyloxyfucoxanthin	But-fuco	Dominant in pelagophytes, dictyochophytes. Present in some haptophytes
Diadinoxanthin	Diadino	Diatoms, haptophytes, pelagophytes, dictyochophytes and some dinoflagellates
Diatoxanthin	Diato	Diatoms, haptophytes, pelagophytes, dictyochophytes and some dinoflagellates
Fucoxanthin	Fuco	Dominant in most red algae
19'-hexanoyloxyfucoxanthin	Hex-fuco	Major in Haptophytes and dinoflagellates Type 2* (lacking Peridinin)
Lutein	Lut	Chlorophytes, prasinophytes
Neoxanthin	Neo	Chlorophytes, prasinophytes
Peridinin	Peri	Dinoflagellates Type 1*
Prasinoxanthin	Pras	Prasinophytes Type 3A and 3B
Violaxanthin	Viola	Dominant in chlorophytes, prasinophytes, chrysophytes, some dinoflagellates
Zeaxanthin	Zea	Dominant in cyanobacteria, pelagophytes, chrysophytes, some dinoflagellates

* Higgins et al. (2011)

BGD
11, 14489–14530, 2014

Table 2. Abundance and carbon biomass (mean ± standard deviation) of the major protist groups in surface and subsurface chlorophyll *a* maximum (SCM) depth of the Mackenzie shelf and deep waters of the Beaufort Sea. The mean percent contribution of each protist group to total cell abundance and total carbon biomass is indicated in parenthesis. Large (> 3 µm) and small (< 3 µm) cells were counted by light microscopy and flow cytometry, respectively. The average cell abundance and carbon biomass are in bold characters. Total chlorophyll *a* concentration (mean ± standard deviation) is indicated at the bottom of the Table. The heterotrophic group is composed of flagellated protozoans.

	Mackenzie Shelf		Beaufort Sea	
Number of stations	Surface (3 m) $N = 8$	SCM (35 ± 8) m $N = 6$	Surface (3 m) $N = 13$	SCM (61 ± 7) m $N = 13$
TOTAL ABUNDANCE (cells mL^{-1})	4500 ± 1400	4000 ± 1500	4400 ± 1400	2500 ± 2500
Algae >3 µm	660 ± 830 (15.0)	3000 ± 900 (74.1)	140 ± 140 (3.2)	93 ± 110 (3.8)
Diatoms	410 ± 610 (61.2)	2900 ± 790 (97.5)	7.1 ± 5.7 (5)	8 ± 11 (8.5)
Dinoflagellates	44 ± 30 (6.6)	8.4 ± 4.8 (0.3)	19 ± 15 (13.1)	11 ± 5 (11.9)
Chlorophytes	0.6 ± 0.9 (0.1)	0.1 ± 0.3 (0)	0.2 ± 0.4 (0.1)	0.0 ± 0.1 (0)
Chrysophytes	36 ± 39 (5.4)	4.9 ± 10.0 (0.2)	5.4 ± 6.3 (3.8)	0.1 ± 0.2 (0.1)
Dictyochophytes	18 ± 28 (2.6)	0.7 ± 1.7 (0)	9.5 ± 9.4 (6.7)	0.5 ± 0.9 (0.5)
Cryptophytes	19 ± 23 (2.8)	5.6 ± 7.0 (0.2)	4.6 ± 5.2 (3.3)	7 ± 20 (7.4)
Euglenophytes	0.2 ± 0.4 (0)	0.1 ± 0.1 (0)	0.2 ± 0.5 (0.1)	0.1 ± 0.1 (0.1)
Prasinophytes	21 ± 27 (3.2)	0.4 ± 0.4 (0)	30 ± 38 (21.2)	0.7 ± 1.5 (0.8)
Prymnesiophytes	15 ± 25 (2.3)	4.0 ± 5.5 (0.1)	19 ± 22 (13.7)	22 ± 25 (24.3)
Unidentified flagellates	100 ± 40 (15.7)	48 ± 36 (1.6)	46 ± 33 (32.8)	37 ± 41 (39.9)
Raphidophytes	0 ± 0 (0)	0.5 ± 0.5 (0)	0.0 ± 0.1 (0)	6.0 ± 6.2 (6.5)
Algae <3 µm	3600 ± 1500 (81.2)	930 ± 850 (23.5)	4000 ± 1200 (91.7)	2200 ± 1300 (91.1)
Heterotrophs >3 µm	40 ± 60 (0.9)	12 ± 14 (0.3)	27 ± 39 (0.6)	2.7 ± 2.4 (0.1)
Unidentified cells >3 µm	120 ± 120 (2.8)	86 ± 44 (2.2)	190 ± 270 (4.4)	120 ± 160 (5.0)

BGD
11, 14489–14530, 2014

Table 2. Continued.

	Mackenzie Shelf		Beaufort Sea	
Number of stations	Surface (3 m) $N = 8$	SCM (35 ± 8) m $N = 6$	Surface (3 m) $N = 13$	SCM (61 ± 7) m $N = 13$
TOTAL BIOMASS (mg C m^{-3})	64 ± 22	110 ± 57	25 ± 7	14 ± 5
Algae >3 µm	43 ± 40 (54.7)	100 ± 46 (86.8)	12 ± 10 (39.5)	9.2 ± 7.6 (48.5)
Diatoms	15 ± 17 (35.9)	91 ± 40 (89.2)	0.51 ± 0.37 (5)	0.31 ± 0.53 (3.8)
Dinoflagellates	23 ± 20 (56.7)	9.7 ± 4.8 (9.5)	7.93 ± 6.49 (76.9)	4.63 ± 3.22 (57.3)
Chlorophytes	0.10 ± 0.21 (0.3)	0.00 ± 0.00 (0)	0.04 ± 0.11 (0.4)	0.00 ± 0.01 (0)
Chrysophytes	0.48 ± 0.33 (1.2)	0.09 ± 0.18 (0.1)	0.32 ± 0.62 (3.2)	0.00 ± 0.01 (0)
Dictyochophytes	0.15 ± 0.24 (0.4)	0.01 ± 0.03 (0)	0.09 ± 0.09 (0.9)	0.00 ± 0.01 (0)
Cryptophytes	0.28 ± 0.33 (0.7)	0.29 ± 0.45 (0.3)	0.04 ± 0.05 (0.4)	0.03 ± 0.06 (0.4)
Euglenophytes	0.04 ± 0.06 (0.1)	0.02 ± 0.04 (0)	0.07 ± 0.16 (0.7)	0.14 ± 0.36 (1.7)
Prasinophytes	0.31 ± 0.35 (0.8)	0.01 ± 0.01 (0)	0.49 ± 0.60 (4.8)	0.02 ± 0.04 (0.2)
Prymnesiophytes	0.13 ± 0.19 (0.3)	0.04 ± 0.05 (0)	0.19 ± 0.21 (1.9)	0.36 ± 0.53 (4.5)
Unidentified flagellates	1.52 ± 0.60 (3.7)	0.57 ± 0.30 (0.6)	0.60 ± 0.40 (5.8)	0.48 ± 0.45 (6)
Raphidophytes	0 ± 0 (0)	0.29 ± 0.29 (0.3)	0.01 ± 0.02 (0.1)	2.10 ± 1.68 (26)
Algae <3 µm	1.9 ± 0.8 (2.4)	0.49 ± 0.45 (0.4)	2.1 ± 0.7 (6.7)	1.2 ± 0.7 (6.2)
Heterotrophs > 3 µm	15 ± 24 (19.3)	5.4 ± 5.6 (4.6)	6.3 ± 10.6 (20.2)	1.0 ± 1.2 (5.3)
Unidentified cells > 3 µm	3.8 ± 4.0 (4.9)	2.3 ± 2.1 (2.0)	4.0 ± 4.4 (12.9)	2.9 ± 3.6 (15.4)
TOTAL Chlorophyll *a* (mg m^{-3})	0.20 ± 0.13	2.84 ± 2.55	0.10 ± 0.09	0.31 ± 0.17

BGD
11, 14489–14530, 2014

Table 3. Pigment : TChl *a* ratios for each algal group under low (SCM samples) and high light (surface samples) levels. (A) Initial ratio matrix determined from 1: This study; 2: Vidussi et al. (2004); 3: Higgins et al. (2011), (B) Final ratio matrix obtained after CHEMTAX recalculation in order to find the best fit between the in situ pigment concentrations and our initial ratio matrix. The symbol "–" indicates similar ratios between low and high light levels. Pigment abbreviations are defined in Table 1. According to Higgins et al. (2011): Chryso-Pelago: Chrysophytes and Pelagophytes; Hapto-7: haptophytes type 7; Prasino-3: prasinophytes type 3; Prasino-2: prasinophytes type 2.

Class / Pigment	Light	Chl c_3	Chl c_{1+2}	But-fuco	Fuco	Hex-fuco	Neo	Pras	Chl *b*	Allo	Lut	Peri
(A) Initial ratio matrix												
[1]Diatoms	Low	0	0.171	0	0.425	0	0	0	0	0	0	0
	High	0	0.192	0	0.495	0	0	0	0	0	0	0
[2]Dinoflagellate	Low	0	0	0	0	0	0	0	0	0	0	0.6
	High	0	0	0	0	0	0	0	0	0	0	0.6
[3]c_3-flagellates	Low	0.262	0.144	0.07	0.226	0.101	0	0	0	0	0	0
	High	0.179	0.126	0.081	0.3	0.194	0	0	0	0	0	0
[3]Cryptophytes	Low	0	0.104	0	0	0	0	0	0	0.277	0	0
	High	0	–	0	0	0	0	0	0	0.211	0	0
[2]Chryso-Pelago	Low	0.114	0.285	0.831	0.337	0	0	0	0	0	0	0
	High	–	0.316	1.165	0.425	0	0	0	0	0	0	0
[3]Hapto-7	Low	0.171	0.276	0.013	0.259	0.491	0	0	0	0	0	0
	High	0.215	0.236	0.023	0.42	0.682	0	0	0	0	0	0
[3]Prasino-2	Low	0	0	0	0	0	0.033	0	0.812	0	0.096	0
	High	0	0	0	0	0	0.056	0	0.786	0	0.038	0
[3]Prasino-3	Low	0	0	0	0	0	0.078	0.248	0.764	0	0.009	0
	High	0	0	0	0	0	0.116	0.241	0.953	0	0.008	0
[3]Chlorophytes	Low	0	0	0	0	0	0.036	0	0.339	0	0.187	0
	High	0	0	0	0	0	0.029	0	0.328	0	0.129	0

BGD
11, 14489–14530, 2014

Table 3. Continued.

Class / Pigment	Light	Chl c_3	Chl c_{1+2}	But-fuco	Fuco	Hex-fuco	Neo	Pras	Chl b	Allo	Lut	Peri
(B) Final ratio matrix												
[1]Diatoms	Low	0	0.091	0	0.301	0	0	0	0	0	0	0
	High	0	0.13	0	0.352	0	0	0	0	0	0	0
[2]Dinoflagellate	Low	0	0	0	0	0	0	0	0	0	0	0.375
	High	0	0	0	0	0	0	0	0	0	0	0.285
[3]c_3-flagellates	Low	0.133	0.072	0.046	0.171	0.11	0	0	0	0	0	0
	High	0.145	0.08	0.039	0.125	0.056	0	0	0	0	0	0
[3]Cryptophytes	Low	0	0.079	0	0	0	0	0	0	0.162	0	0
	High	0	0.075	0	0	0	0	0	0	0.201	0	0
[2]Chryso-Pelago	Low	0.038	0.105	0.386	0.141	0	0	0	0	0	0	0
	High	0.044	0.111	0.324	0.131	0	0	0	0	0	0	0
[3]Hapto-7	Low	0.079	0.071	0.008	0.154	0.321	0	0	0	0	0	0
	High	0.036	0.061	0.006	0.122	0.303	0	0	0	0	0	0
[3]Prasino-2	Low	0	0	0	0	0	0.03	0	0.424	0	0.02	0
	High	0	0	0	0	0	0.017	0	0.418	0	0.049	0
[3]Prasino-3	Low	0	0	0	0	0	0.054	0.209	0.271	0	0.004	0
	High	0	0	0	0	0	0.043	0.136	0.222	0	0.005	0
[3]Chlorophytes	Low	0	0	0	0	0	0.035	0	0.037	0	0.143	0
	High	0	0	0	0	0	0.023	0	0.217	0	0.12	0

BGD
11, 14489–14530, 2014

Table 4. Physical, chemical and biological characteristics (mean + standard deviation) for each cluster presented in Fig. 4. The cluster 1 is subdivided for samples collected in surface water (surf) and sub-surface chlorophyll maximum (SCM) depth. PAR: Percentage of the surface photosynthetically active radiation: C/TChl *a*: ratio of algal carbon biomass to total chlorophyll *a* concentration (i.e. TChl *a* = Chl *a* + Chlid *a*).

	Depth (m)	*T* (°C)	Salinity	PAR ($\mu M\,m^{-2}\,s^{-1}$)	NO_3^- ($\mu mol\,L^{-1}$)	NH_4^+ ($\mu mol\,L^{-1}$)	PO_4^{3-} ($\mu mol\,L^{-1}$)	TChl *a* ($\mu g\,L^{-1}$)	C/TChl *a*
Cluster 1 ($n = 11$)	24 ± 16	0.8 ± 2.7	30.2 ± 3.0	39 ± 78	3.1 ± 2.8	0.09 ± 0.11	0.96 ± 0.41	1.80 ± 2.35	140 ± 150
Cluster 1 surf ($n = 4$)	5 ± 3	4.2 ± 1.1	26.7 ± 3.7	100 ± 110	0.2 ± 0.2	0.01 ± 0.01	0.50 ± 0.14	0.16 ± 0.04	280 ± 150
Cluster 1 SCM ($n = 7$)	35 ± 8	−1.0 ± 0.1	31.7 ± 0.4	2.2 ± 2.3	5.1 ± 1.6	0.15 ± 0.12	1.27 ± 0.11	2.73 ± 2.55	49 ± 23
Cluster 2 (n=15)	2 ± 1	3.7 ± 2.9	24.1 ± 6.4	129 ± 85	0.1 ± 0.1	0.02 ± 0.04	0.54 ± 0.10	0.12 ± 0.13	160 ± 110
Cluster 3 (n=8)	66 ± 4	−1.1 ± 0.1	31.5 ± 0.2	2.2 ± 1.2	5.1 ± 2.7	0.02 ± 0.02	1.26 ± 0.20	0.28 ± 0.16	38 ± 23
Cluster 4 (n=6)	56 ± 5	−1.1 ± 0.1	31.0 ± 0.4	4.7 ± 1.7	0.5 ± 0.2	0.03 ± 0.02	0.86 ± 0.06	0.36 ± 0.20	34 ± 25

BGD
11, 14489–14530, 2014

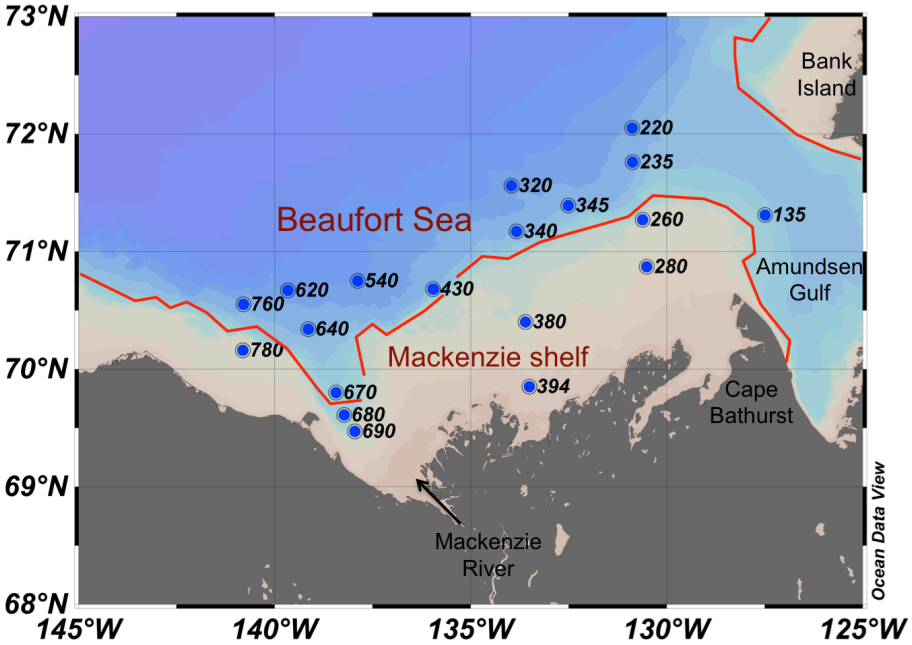

Figure 1. Location of the sampling stations in the Canadian Beaufort Sea from 30 July to 27 August 2009 during the MALINA expedition. The isobath 150 m (in red) separates the Mackenzie shelf from the deep waters of the Beaufort Sea.

BGD
11, 14489–14530, 2014

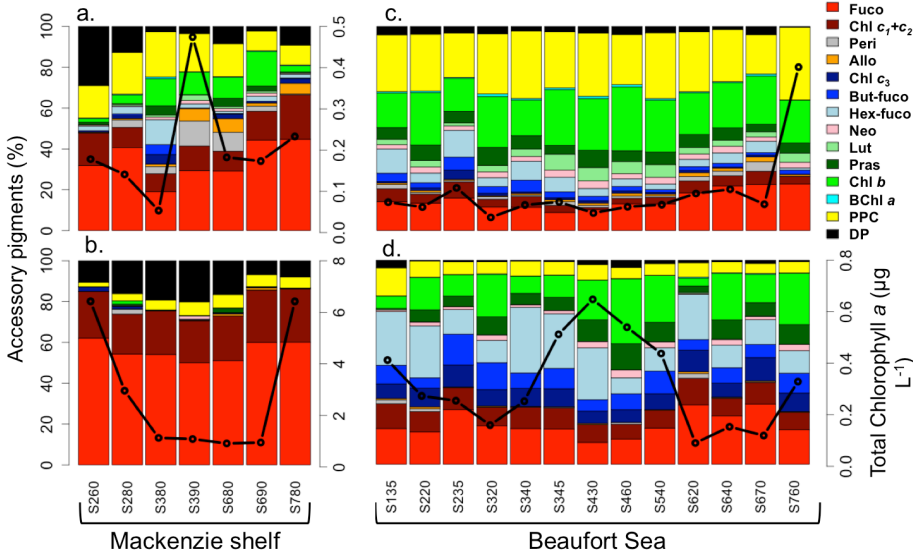

Figure 2. Relative contribution of accessory pigments to total accessory pigment (wt : wt) in **(a, c)** surface water and at the **(b, d)** sub-surface chlorophyll maximum (SCM) depth of the **(a, b)** Mackenzie shelf and **(c, d)** deep waters of the Beaufort Sea. The black line with circle represents the chlorophyll *a* concentration. DP: degradation pigments (Chlide *a* + Pheide *a* + Phe *a*); PPC: photoprotective carotenoids (i.e. Diadino + Diato + Zea + Viola + Car). Pigment abbreviations are defined in Table 1.

BGD
11, 14489–14530, 2014

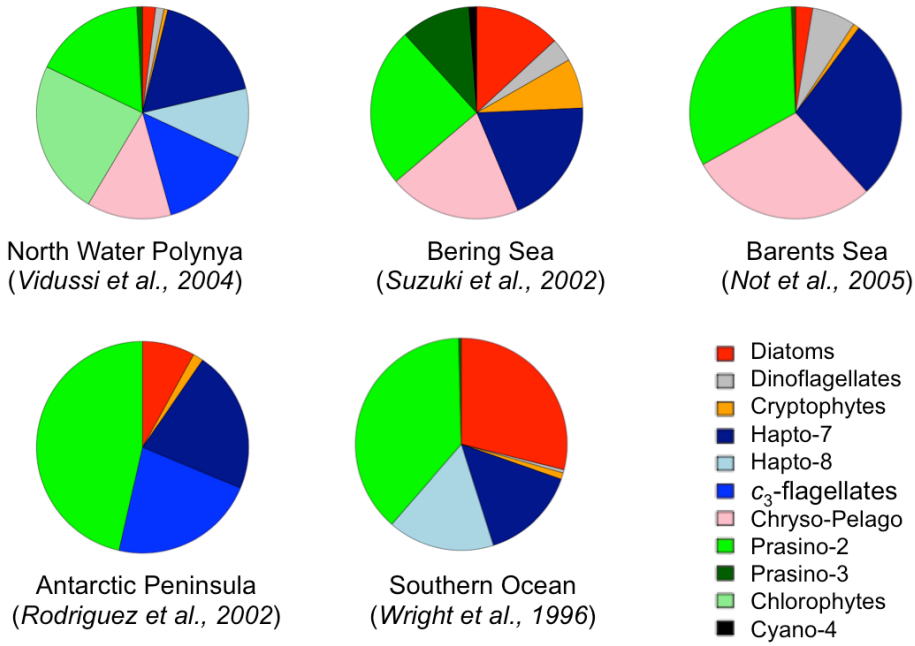

Figure 3. Average contribution of major algal groups to total chlorophyll *a* (Chl *a*) concentration at the sub-surface chlorophyll maximum (SCM) depth in the deep waters of the Beaufort Sea calculated with the CHEMTAX software using five different pigment/Chl *a* ratio matrices. Ratio matrices are from previous studies conducted in polar oceans: Vidussi et al. (2004) in North Water Polynya, Suzuki et al. (2002) in Bering Sea, Not et al. (2005) in Barents Sea, Rodriguez et al. (2002) in Antarctic Peninsula and Wright et al. (1996) in Southern Ocean. According to Higgins et al. (2011): Hapto-7: haptophytes type 7; Hapto-8: haptophytes type 8; Chryso-Pelago: Chrysophytes and Pelagophytes; Prasino-2: prasinophytes type 2; Prasino-3: prasinophytes type 3; Cyano-4: cyanobacteria type 4.

BGD
11, 14489–14530, 2014

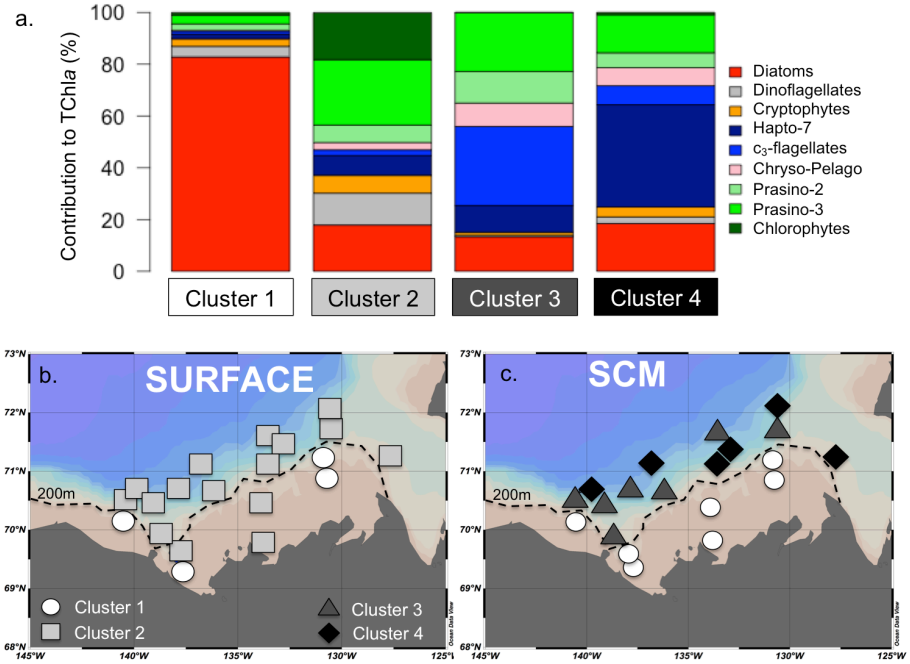

Figure 4. (a) Relative contribution of major algal groups to total chlorophyll *a* (Chl *a*) concentration (calculated by CHEMTAX) for four groups of samples with similar pigment composition (clusters) determined with the k-means clustering method (MacQueen, 1967). The geographical position of the four groups of samples (4 clusters) is mapped for the **(b)** surface water and **(c)** sub-surface chlorophyll maximum (SCM) depth. According to Higgins et al. (2011): Hapto-7: haptophytes type 7; Chryso-Pelago: Chrysophytes and Pelagophytes; Prasino-2: prasinophytes type 2; Prasino-3: prasinophytes type 3.

BGD
11, 14489–14530, 2014

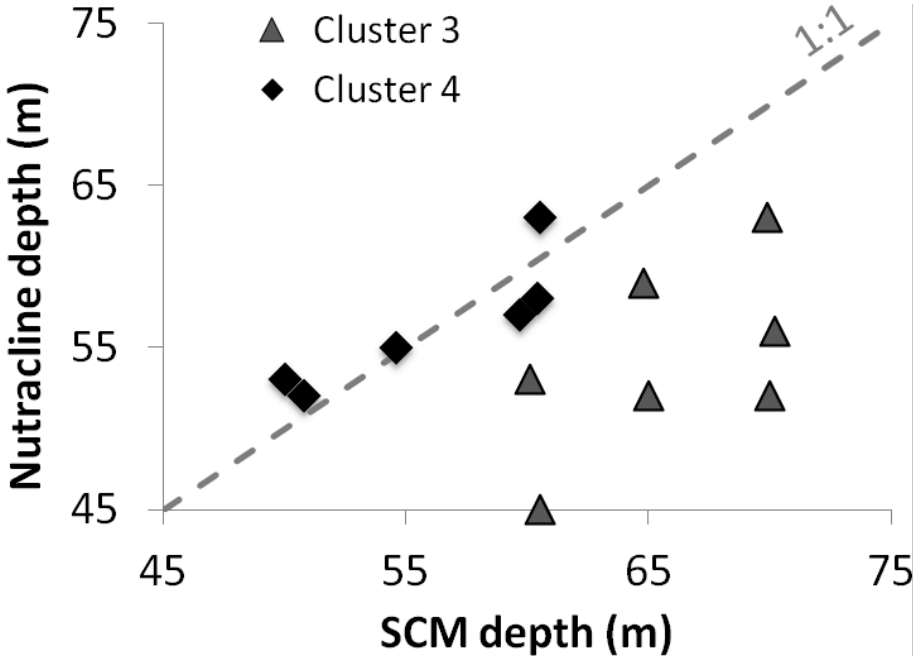

Figure 5. Relationship between the nitracline depth and the sub-surface chlorophyll *a* maximum (SCM) depth for samples of clusters 3 (grey triangle) and 4 (black diamond). The dashed line represents a 1:1 relationship. Note the SCM depth matches with the nitracline depth for cluster 4 samples. In contrast, the SCM is deeper than the nitracline depth for cluster 3 samples.

BGD
11, 14489–14530, 2014

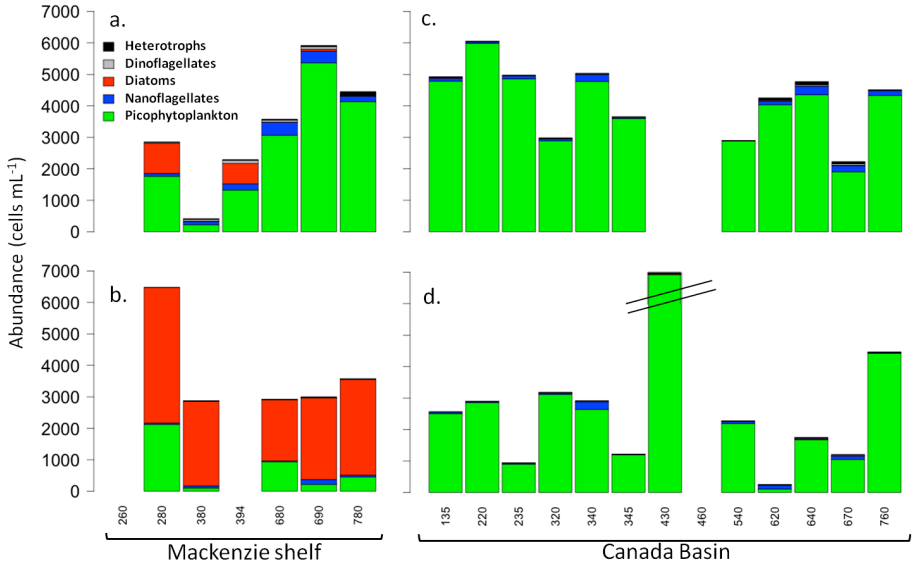

Figure 6. Abundance of five protist groups in **(a, c)** surface and at the **(b, d)** subsurface chlorophyll maximum (SCM) depth of the **(a, b)** Mackenzie shelf and **(c, d)** deep waters of the Beaufort Sea.

BGD
11, 14489–14530, 2014

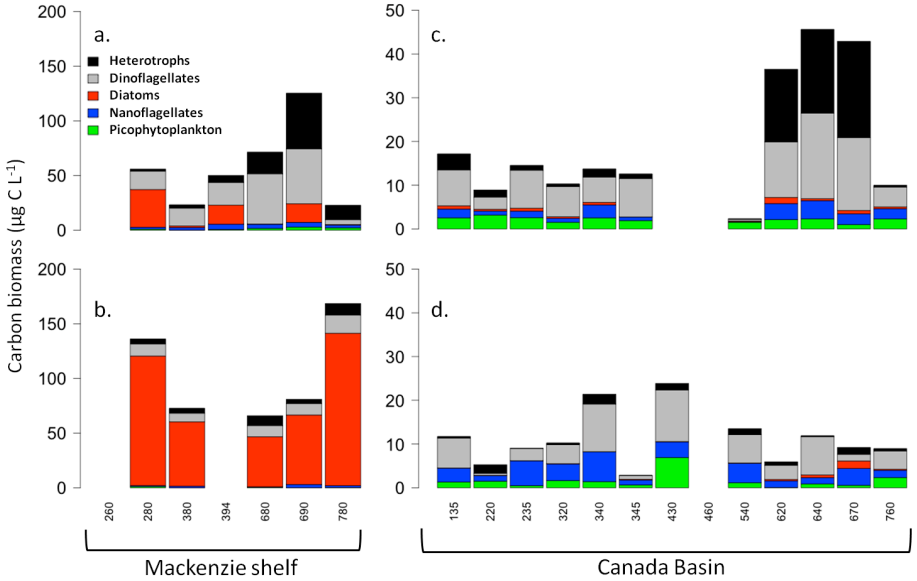

Figure 7. Carbon biomass of five protist groups in **(a, c)** surface and at the **(b, d)** subsurface chlorophyll maximum (SCM) depth of the **(a, b)** Mackenzie shelf and **(c, d)** deep waters of the Beaufort Sea.

BGD
11, 14489–14530, 2014

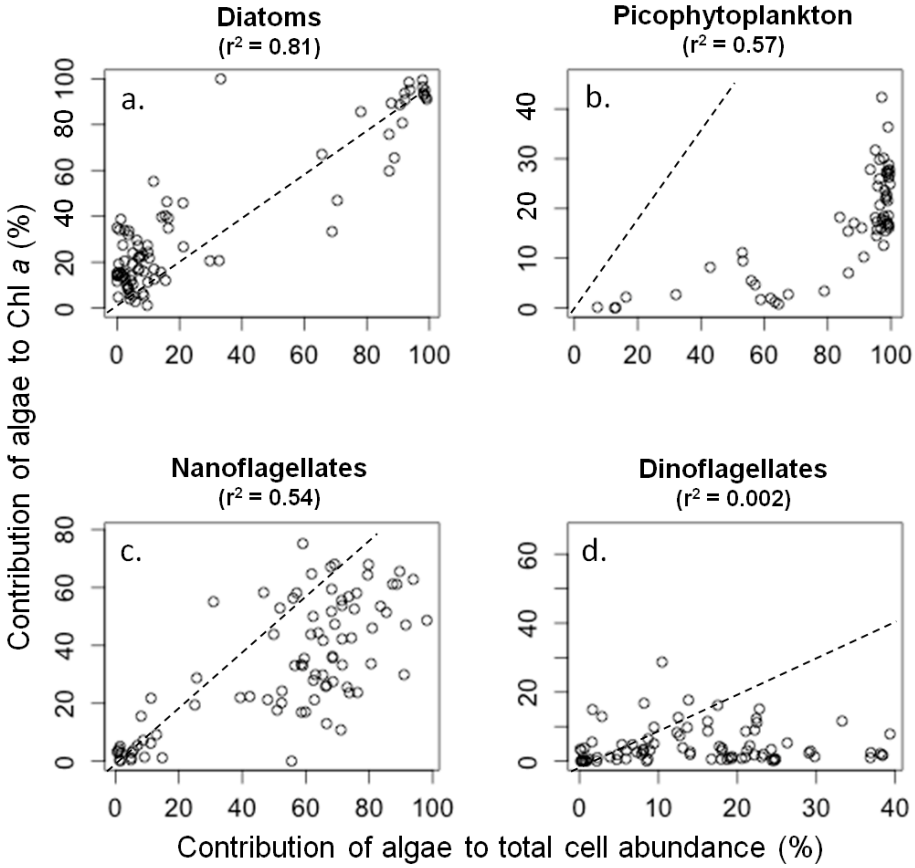

Figure 8. Scatter diagrams of the contribution of **(a)** diatoms, **(b)** picophytoplankton, **(c)** nanoflagellates and **(d)** dinoflagellates to total chlorophyll *a* (Chl *a*) concentration (calculated by CHEMTAX) as a function of their contribution to total cell abundance. The dashed line represents the 1 : 1 relationship. The Pearson correlation coefficient (r^2) is indicated for each algal group.

BGD
11, 14489–14530, 2014

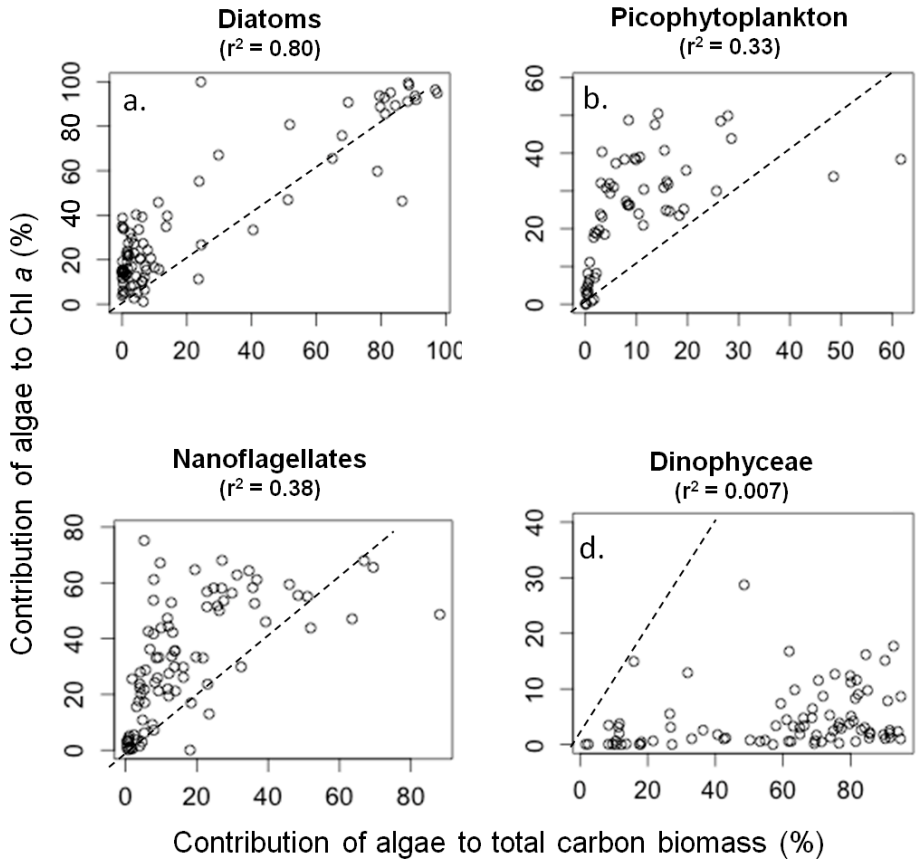

Figure 9. Scatter diagrams of the contribution of **(a)** diatoms, **(b)** picophytoplankton, **(c)** nanoflagellates and **(d)** dinoflagellates to total chlorophyll *a* (Chl *a*) concentration (calculated by CHEMTAX) as a function of their contribution to total carbon biomass (calculated from biovolume, see Materials and methods). The dashed line represents the 1:1 relationship. The Pearson correlation coefficient (r^2) is indicated for each algal group.

BGD
11, 14489–14530, 2014